Available online at www.sciencedirect.com
SCIENCE DIRECT®
International Journal of Thermal Sciences 43 (2004) 453–463
International Journal of Thermal Sciences
www.elsevier.com/locate/ijts

Thermal diffusivity measurement in slabs using harmonic and one-dimensional propagation of thermal waves

Alberto Muscio [a,*], Paolo G. Bison [b], Sergio Marinetti [b], Ermanno Grinzato [b]

[a] *DIMeC—Dipartimento di Ingegneria Meccanica e Civile, Università di Modena e Reggio Emilia, Via Vignolese, 905/B, 41100 Modena, Italy*
[b] *CNR-ITC Padova section, Corso Stati Uniti, 4, 35127 Padova, Italy*

Received 9 September 2002; accepted 15 October 2003

Abstract

The development of a novel approach to the well-known Ångström's method for the measurement of the thermal diffusivity is reported. In this method, the diffusivity is determined from the damping and the phase shift of a periodic thermal signal during its propagation along the specimen. The propagation can be easily monitored by infrared thermography. In general, a non-contact source is used to apply the signal.

In the present work, however, a direct-contact source is employed, with a temperature-oscillation signal supplied on a portion of one of the two main surfaces of the specimen, where a homogeneous contact can be yielded by using a proper contact pressure. Such practice implies that the measures of surface temperature can be used to estimate the diffusivity only beyond a certain distance from the source, where the wave-front of the temperature oscillation within the specimen becomes plane and perpendicular to the main surfaces. This distance is investigated here, to establish a general rule for the performance of the experiments.

A thermoelectric device based on the Peltier effect is employed as the thermal source. The main difficulty about its use is to obtain a perfectly harmonic and well-balanced thermal signal. This is necessary to avoid a complex processing of the experimental data, and it can be achieved by supplying a current with a properly-chosen time-evolution pattern. Such an approach, which is built upon previous work, is here enhanced by improving the underlying analytical model.

Keywords: Thermal diffusivity; Measurement; Ångström's method; Infrared thermography; Peltier effect

1. Introduction

The development of a novel approach to the well-known Ångström's method for the measurement of the thermal diffusivity is reported. This is based on supplying to a slab specimen a periodic thermal signal with null net input [1]. The thermal diffusivity of the tested material is determined from the damping and the phase shift of the thermal signal during its propagation along the specimen. The propagation can be easily monitored by infrared thermography.

The aim is to overcome some limitations of the most utilized standard test methods, the guarded-hot-plate and the laser flash, when these are used to characterize thin specimens with high conductivity or diffusivity. In particular, a greater accuracy is sought than the guarded-hot-plate, while using a simpler experimental procedure than the laser flash.

A harmonic thermal signal is used, with null net heat input. In other words, a harmonic temperature oscillation around the ambient value is imposed onto the surface of the specimen.

The specimen has the shape of a long thin slab and the temperature oscillation is imposed on a strip of one of its two main surfaces. When the temperature oscillation propagates within the specimen from that strip, its wave-front is initially plane and parallel to the main surfaces. Hereafter, it starts bending and becoming more and more curved until, above a certain distance, a plane wave-front is achieved again, at another time. However, this is no more parallel but perpendicular to the surfaces, so that the thermal signal is now propagating aside of the input strip, along the main dimension of the specimen.

At the end, a perfectly harmonic and one-dimensional temperature oscillation is obtained within the specimen. Its

* Corresponding author.
E-mail addresses: alberto.muscio@unimore.it (A. Muscio), paolo.bison@itc.cnr.it (P.G. Bison), sergio.marinetti@itc.cnr.it (S. Marinetti), ermanno.grinzato@itc.cnr.it (E. Grinzato).

1290-0729/$ – see front matter
doi:10.1016/j.ijthermalsci.2003.10.005

Nomenclature

Latin symbols

A	input surface area	m^2
a	Seebeck coefficient	$V \cdot K^{-1}$
C	heat capacity	$J \cdot K^{-1}$
c	specific heat capacity	$J \cdot (kg \cdot K)^{-1}$
d	specimen thickness	m
G	shape factor of a pellet	m
h	convective heat transfer coefficient	$W \cdot (m^2 \cdot K)^{-1}$
I	electric current	A
k	thermal conductivity	$W \cdot (m \cdot K)^{-1}$
L	thermal diffusion length	m
N	number of couples in a thermoelectric module	
Q	heat rate	W
r	electrical resistivity	$\Omega \cdot m$
S	cross-section area of a pellet	m^2
s	height of a pellet	m
T	temperature	K
t	time	s
t_0	period of the temperature oscillation	s
t_e	external relaxation time	s
x	longitudinal coordinate (distance from the thermal source)	m
$x_{accessible}$	extension of the optically accessible surface	m
x_{strip}	extension of the thermal input (strip) surface	m
z	depth coordinate (distance from the accessible surface)	m

Greek symbols

α	actual thermal diffusivity	$m^2 \cdot s^{-1}$
α_β	apparent thermal diffusivity from wave phase	$m^2 \cdot s^{-1}$
α_γ	apparent thermal diffusivity from wave damping	$m^2 \cdot s^{-1}$
β	phase-modifying factor due to convective heat transfer	
γ	amplitude-modifying factor due to convective heat transfer	
ΔT	temperature difference across a thermoelectric module	K
ΔT_x	local amplitude of the temperature oscillation	K
ΔT_0	maximum amplitude of the temperature oscillation	K
ρ	mass density	$kg \cdot m^{-3}$
φ_x	local phase shift of the temperature oscillation	rad
φ_0	initial phase of the temperature oscillation	rad

Subscripts

a	ambient
c	cold side
h	hot side
s	specimen
x	at the x-location

phase-shift and damping can be monitored by measuring the temperature on the specimen surface. Then, these can be correlated to the thermal-diffusivity value through simple analytical formulas.

The experimental implementation of the proposed measurement method is investigated in depth in this work, in which the focus is on the practice to obtain a thermal signal both one-dimensional and perfectly harmonic.

2. The measurement method

The measurement method, although well known, is succinctly introduced for the sake of completeness. A more detailed description is reported in [1,2].

The implementation of the method presented here is targeted to measure the thermal diffusivity of a thin slab made of a homogeneous material. A thermoelectric source supplies a periodic thermal input to a 'strip' of the slab surface. The strip is in the middle of the slab and covers the whole width. The remaining surface is exposed to ambient air and is optically accessible (see Fig. 1).

Neglecting the side effects, the problem can be considered two-dimensional in the x–z plane. Symmetry also exists about the vertical mid-plane. Therefore, only half of the specimen needs to be considered. The heat diffusion problem in the slab is governed by the Fourier's equation with no generation term:

$$\frac{\partial T}{\partial t} = \alpha\left(\frac{\partial^2 T}{\partial x^2} + \frac{\partial^2 T}{\partial z^2}\right) \tag{1}$$

Because of the thermoelectric device, the boundary condition for the thermal input surface consists in a harmonic temperature oscillation around the ambient temperature:

$$T(-x_{strip} \leqslant x \leqslant 0,\ z = 0,\ t) = T_a + \Delta T_0 \sin\left(2\pi \frac{t}{t_0} - \varphi_0\right) \tag{2}$$

where x_{strip} is the x-dimension of the input surface strip (see Fig. 1), t_0 is the oscillation period, ΔT_0 is the maximum oscillation amplitude and φ_0 is the initial phase.

Other boundary conditions are those of null heat flux at the symmetry plane and convective-radiative heat transfer elsewhere.

The initial temperature is assumed uniform in the slab and equal to the ambient value, T_a. The initial condition, however, has an effect on the initial transient only, but not on the long-term steady-periodic response of the system [3].

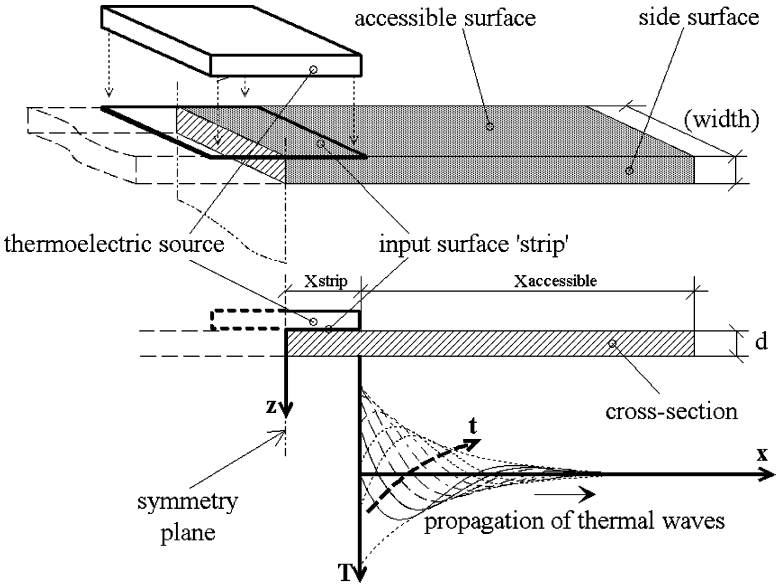

Fig. 1. Slab specimen and thermal source.

A further simplification of the model is possible if the temperature across the slab thickness, d, is almost uniform at any x-location. This occurs only beyond a given distance from the source, for which one can set $x = 0$. Hereafter, the thermal waves induced by the source propagate along the slab as a plane front, so that the slab becomes thermally similar to a long thin rod. The governing equation thus is:

$$\frac{\partial T}{\partial t} = \alpha \frac{\partial^2 T}{\partial x^2} - \frac{2h}{\rho c d}(T - T_a) \tag{3}$$

If the slab is long enough, the temperature oscillations are almost completely damped before reaching the far edge. In this case, the rod can be considered semi-infinite, i.e., $x_{\text{accessible}} \to \infty$ in Fig. 1.

The boundary conditions for the one-dimensional model are:

$$T(x = 0,\ t) = T_a + \Delta T_0 \sin\left(2\pi \frac{t}{t_0} - \varphi_0\right) \tag{4}$$

$$T(x \to \infty,\ t) = T_a \tag{5}$$

Beyond the distance at which the wave-front of the temperature oscillations becomes plane and perpendicular to the main surfaces of the specimen, a long-term ($t \to \infty$) steady-periodic analytical solution is available for the system of Eqs. (3)–(5), independent of the initial condition [3]:

$$T(x, t) = T_a + \Delta T_0 \mathrm{e}^{-\gamma \frac{x}{L}} \sin\left(2\pi \frac{t}{t_0} - \beta \frac{x}{L} - \varphi_0\right) \tag{6}$$

where

$$\beta = \sqrt{-\frac{1}{2\pi}\frac{t_0}{t_e} + \sqrt{1 + \left(\frac{1}{2\pi}\frac{t_0}{t_e}\right)^2}} \tag{7}$$

$$\gamma = \sqrt{\frac{1}{2\pi}\frac{t_0}{t_e} + \sqrt{1 + \left(\frac{1}{2\pi}\frac{t_0}{t_e}\right)^2}} \tag{8}$$

The 'thermal diffusion length' L is a characteristic parameter of the thermal problem and it is defined as follows:

$$L = \sqrt{\frac{\alpha t_0}{\pi}} \tag{9}$$

The time t_e in Eqs. (7)–(8) is known as the 'external relaxation time', and it is defined as:

$$t_e = \frac{\rho c d}{2h} \tag{10}$$

When t_e is much larger than t_0, heat transfer by convection between the slab and the environment is negligible with respect to the heat diffusion within the solid. Therefore, the last term in Eq. (3) can be neglected. The solution for negligible convection is thus obtained [3]:

$$T(x, t) = T_a + \Delta T_0 \mathrm{e}^{-\frac{x}{L}} \sin\left(2\pi \frac{t}{t_0} - \frac{x}{L} - \varphi_0\right) \tag{11}$$

However, when using a low-frequency source like the thermoelectric heat pumps considered here, convection is usually significant and Eq. (6) must be used.

Both Eq. (6) and Eq. (11) are obtained under the assumption of planar symmetry of the test system. This is achieved by placing the thermal source centrally on the specimen surface. An asymmetrical position of the source, however, is not expected to affect the solutions, provided that the length of the shorter part of the specimen is greater than a few times L.

Different procedures may be used for the estimation of the diffusivity, such as inverse analysis techniques, non-linear fitting of Eq. (6), or the approach eployed here, a classical linear least-square estimation applied to the phase lag and the exponentially decaying amplitude of the thermal waves. This relatively simple approach is made possible by applying a perfectly harmonic thermal signal with null net heat input. In fact, finding out the practice to obtain that signal is the purpose of this work.

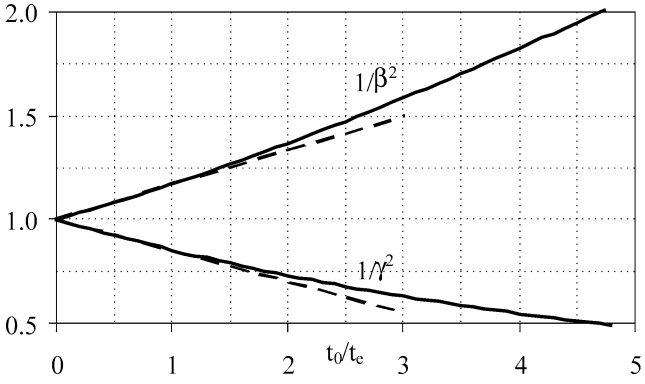

Fig. 2. Behavior of factors $1/\beta^2$ and $1/\gamma^2$ versus t_0/t_e.

From the phase lag, one can calculate an apparent value of the thermal diffusivity, α_β, that is related to the actual value, α, by an unknown factor depending on convection:

$$\alpha_\beta = \alpha \frac{1}{\beta^2} \tag{12}$$

Another apparent value of the thermal diffusivity, α_γ, can be calculated from the wave amplitude, also this one related to the actual value by an unknown factor:

$$\alpha_\gamma = \alpha \frac{1}{\gamma^2} \tag{13}$$

The actual diffusivity is respectively overestimated ($1/\beta^2 > 1$) or underestimated ($1/\gamma^2 < 1$). In both cases, the discrepancy depends on the ratio t_0/t_e and, consequently, on the convection coefficient. Fig. 2 reveals, however, that the overestimate by using the linear fitting of the phase lag, Eq. (12), is negligible if t_0 is much smaller than t_e, and that the same applies to the underestimate by using the linear fitting of the wave amplitude, Eq. (13). Convection can thus be neglected and the apparent diffusivity coincides with the actual diffusivity. Unfortunately, the condition occurs only when thin specimens of high-diffusivity materials are tested. In the other cases, however, combining α_β and α_γ from the same experiment would allow to determine the true value of the diffusivity [3–7]:

$$\alpha = \sqrt{\alpha_\beta \cdot \alpha_\gamma} \tag{14}$$

An experimental apparatus based on the above-described approach was implemented at the CNR-ITC in Padova [1, 2,6,7]. A liquid-cooled thermoelectric source, driven by a computer-controlled power supply, was used to apply the thermal input. A high-resolution Agema Thermovision® 900 thermographic camera [8] measured the surface temperature of the specimen.

The diffusivity value was determined from the surface-temperature data through the procedure that is summarized below.

(a) Preliminary data reduction.

The raw temperature data are arranged in a matrix. Each column represents the behavior of a pixel on the sample surface in time. Each row is the spatial temperature profile of the sample surface at a given time and is the average of several adjacent lines of the original thermal image. This first step of the data reduction permits to achieve a typical standard deviation ranging from 0.02 K for a last generation sensor to 0.2 K typical of older equipment. Thereafter, the estimation procedure is divided into two more steps: fitting in time and fitting in space.

(b) Fitting in time.

Each column of the matrix is fitted through a least square procedure by a harmonic function of time. Notwithstanding sine and cosine are transcendental functions, the least square procedure is linear as the model is linear in the parameters amplitude and phase which are the results of this stage. The error associated to the estimation is also given together with the test of χ^2 for the goodness of fit. Only the parameters obtained from a good fit are retained for the successive spatial fitting. It should be clear that a good fit is generally obtained close to the source, where the signal is high, while the fit is less reliable in spatial positions far from the source, where the noise dominates.

In a typical experiment, the time step between two successive sampling is 1 to 10 s depending on the period of the heating source. The acquisition lasts for one or more cycles of the thermal source, producing some hundreds sample in time.

(c) Fitting in space

The amplitude as a function of space is damped exponentially, therefore its logarithm is a straight line whose slope depends on thermal diffusivity. The phase changes linearly with space and its slope depends on thermal diffusivity also. The errors associated with the estimations of the two slopes are considered as well. In a typical experiment, a pixel covers one square millimeter area of the sample. More than 200 pixels are taken into account in the spatial fitting, along the heat propagation direction. Only a fraction (say 50–100) is meaningful as the thermal signal is highly damped in space, and that fraction is selected on the base of the aforementioned χ^2 criterion.

(d) Final estimate.

The final result for thermal diffusivity comes from the combination of the two estimated slopes. The propagation of errors from the original temperature data through the various fitting steps down to the final results is computed according to classical rules and good practice of data and error analysis.

The experiments were conducted on one slab made of AISI-304 steel ($\alpha = 3.99 \times 10^{-6}$ $m^2 \cdot s^{-1}$ measured by Laser Flash [6,7]). To obtain a statistical validation of the method, 38 tests were carried out. Varying parameters were the period of the thermal wave, its amplitude and the convective condition (tested with vertical or horizontal specimen, natural and forced convection). Data are reported in Fig. 3 with error bar corresponding to $+/-$ one standard deviation.

Overall, the results were very encouraging. A few technical issues, however, were evidenced by the experiments. Among these, the most critical ones are:

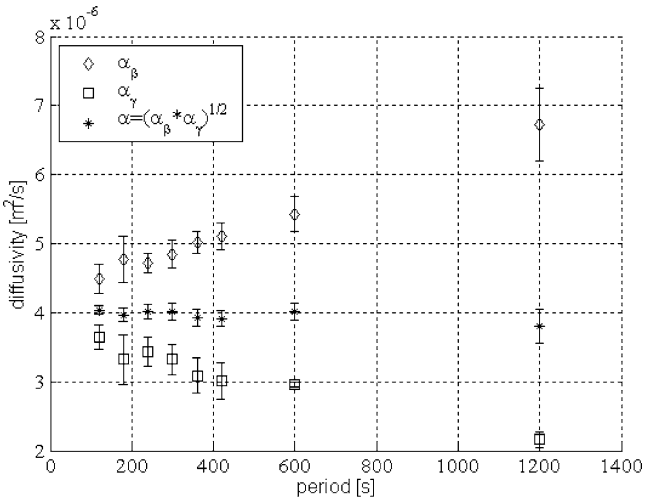

Fig. 3. Diffusivity values obtained from several experiments on AISI-304 specimen.

(a) obtaining a proper thermal input, perfectly-harmonic and with null net heat flux;
(b) determining the distance from the thermal source, beyond which the wave propagation can be considered one-dimensional.

Both subjects are analyzed in the following paragraphs.

3. Harmonic thermal signal with null net heat input

A null net input of the thermal signal is needed, in order to set the average temperature of the specimen to the desired value, namely the ambient temperature. If a non-zero direct component occurs in the signal, the equilibrium value about which the temperature oscillates differs from the temperature of the test ambient, and is inhomogeneous all over the specimen. Moreover, the direct component must be de-coupled from the periodic component.

The thermal signal should also be perfectly harmonic. In fact, while it is usually possible to develop a periodic but non-harmonic signal into a Fourier's series of harmonic components, a complex processing of the distribution and evolution of the surface temperature is required to separate the contribution of each component. Instead, a harmonic thermal signal, with negligible high-order components, allows recovering the diffusivity value by a simple processing of the experimental data.

In previous studies on AC calorimetric and wave-propagation methods, the techniques originated by the Ångström's method, non-contact sources were usually employed such as light or laser beams chopped by a moving mask [9–15]. These are relatively practical to use, but yield a positive net input of the thermal signal, which can shift significantly the reference temperature of the experiment and must be adequately filtered. Moreover, strong high-order harmonics often arise.

Complicated techniques can be employed to obtain a null net heat input, such as alternating flows of hot and cold fluids (the method actually adopted by Ångström). The most practical way, however, may consist in using a thermoelectric device based on the Peltier effect, set in contact with the specimen. In fact, this device pumps heat when a direct current flows through it, and it can alternate heating and cooling stages by simply switching the direction of the current. Such an approach was tested by a few authors [16–18] with positive outcomes, and it was adopted in the set-up of the method investigated here [19]. Its enhancement is the main contribution of the present work.

The dynamic behavior of a thermoelectric device is strongly non-linear. Therefore, even if it is supplied with a harmonic current input, the thermal output is far from being harmonic and well-balanced. An immediate solution to this seems to be the adoption of a closed-loop controller based on a temperature sensor. Unfortunately, design and calibration of controllers of this type are quite complex [20] and can result impractical for material testing, with regard to the ease and the rapidity of the experiment. Moreover, the feedback system requires temperature probes such as thermocouples, which can easily be insufficiently accurate for small temperature oscillations and must be small enough to avoid perturbations in the thermal field. Other types of sensor can be too slow for high-frequency oscillations.

For these reasons, an original strategy of use of the thermoelectric source has been developed. The thermal signal is generated by supplying a current input with a properly-chosen time-evolution pattern, and there is no need of a real-time feed-back loop. The pattern is developed from the analytical formula that governs the transient behavior of a thermoelectric device and its thermal load.

This method was experimentally tested in a preliminary form with satisfactory results [1,2,4–7,19]. Here, it is enhanced by improving the analytical model from which the time-evolution pattern of the current is obtained. From the improved model, a pattern is developed for the current supply, by which an optimal thermal input can theoretically be provided.

An elementary thermoelectric module is made-up by bridging electrically the extremities of two prismatic legs (the pellets) made of p- and n-type semiconductor material, usually bismuth telluride (Bi_2Te_3). At one end the pellets are contacted by a copper tab, the 'cold junction'. A p-type/metal/n-type dual heterojunction structure is thus formed. The opposite ends are contacted by two distinct, mutually insulated, copper tabs, the 'hot junctions'.

In a commercial thermoelectric module, several elementary modules are serially interconnected, as sketched in Fig. 4. The assembly of semiconductor couples is sandwiched between two thin plates of high-purity ceramics (alumina), working as electrical insulators.

A thermoelectric module operates in cooling mode if an electrical current I is supplied. When passing through the cold junctions, the electrons absorb energy from these to

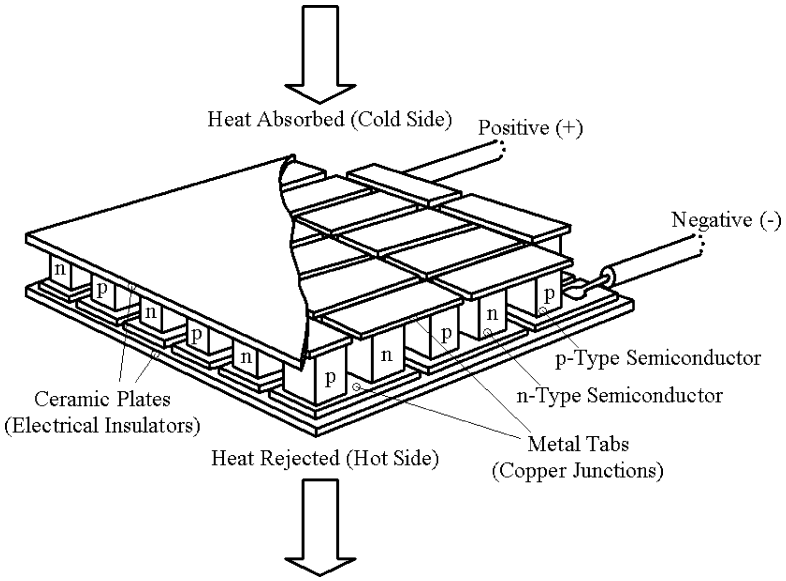

Fig. 4. Sketch of a commercial thermoelectric module.

overcome the local potential step. The opposite occurs at the hot junctions, due to the opposite sign of the potential step. With this Peltier effect, heat is transferred by the electron current across the module, being subtracted to one of the plates and rejected to the other. A temperature difference $\Delta T = T_\mathrm{h} - T_\mathrm{c}$ is finally established between the two opposite sides, with the hot junctions being usually kept at a temperature close to the ambient value by a proper heat sink.

The total cooling power, Q_c, of a device consisting in N serially-interconnected thermoelectric couples is given by the following well known formula [21]:

$$Q_\mathrm{c} = 2N\left[a(T_h - \Delta T)I - \frac{1}{2}\frac{r}{G}I^2 - Gk\Delta T\right] \tag{15}$$

where a, r, and k are, respectively, the Seebeck coefficient, the electrical resistivity and the thermal conductivity of the semiconductor. The shape factor, G, is defined as $G = S/s$, where S is the pellet cross-section area, and s is the pellet height.

Eq. (15) is illustrative of the non-linear behavior of thermoelectric devices. This is such that supplying a sinusoidal voltage or current input produces a temperature cycle significantly distorted with respect to a perfectly-harmonic one. This is shown in Fig. 5, which represents the time-evolution of $\Delta T = T_\mathrm{a} - T_\mathrm{c}$ predicted for a harmonic current input with zero mean value by a fully numerical model of the thermoelectric module.

Even if a null external heat load is assumed, the comparison with a reference harmonic cycle with the same amplitude evidences distortions. Moreover, the temperature oscillates about a value that is well above the ambient one (zero in the normalized scale of Fig. 5), due to the opposed contribution of the Joule dissipation between cooling and heating.

A more balanced thermal disturbance is achieved by supplying a current cycle with above-zero mean value (with a positive current being equivalent to cooling), or different amplitudes in heating and cooling. An initial guess can be made for the mean value, then it can be improved looking at the experimental results. The thermal disturbances calculated numerically for this approach is illustrated in Fig. 6.

Again the comparison with a reference harmonic cycle shows that the signal is distorted, but the mean value can be set to zero. Much better results are however obtained by supplying a current cycle with different amplitudes in heating and cooling. A proper choice of the amplitude ratio, which is also in this case attainable through an initial guess and a subsequent experimental optimization, can produce an undeniably good thermal signal, as depicted in Fig. 7.

In view of the ease of implementation, the latter control strategy is acceptable whenever the easy set up of the experiments is mostly desired, and it was actually adopted in the early laboratory experiences [4,5,19]. However, the selection of the proper amplitude ratio must be performed by 'trial and error', and this can be a time-consuming operation.

The problem of obtaining a truly-harmonic thermal disturbance without the need of either a real-time feedback or a troublesome calibration of the thermal source can be ultimately overcome by using a current cycle with proper time-evolution pattern. This is determined by solving Eq. (15) with respect to I (current) and then imposing a harmonic oscillation of the temperature at the cold side of the thermoelectric module. To the purpose, Eq. (15) can be rewritten as follows:

$$\frac{1}{2}\frac{r}{G}I^2 - a(T_\mathrm{h} - \Delta T)I + kG\Delta T + \frac{Q_\mathrm{c}}{2N} = 0 \tag{16}$$

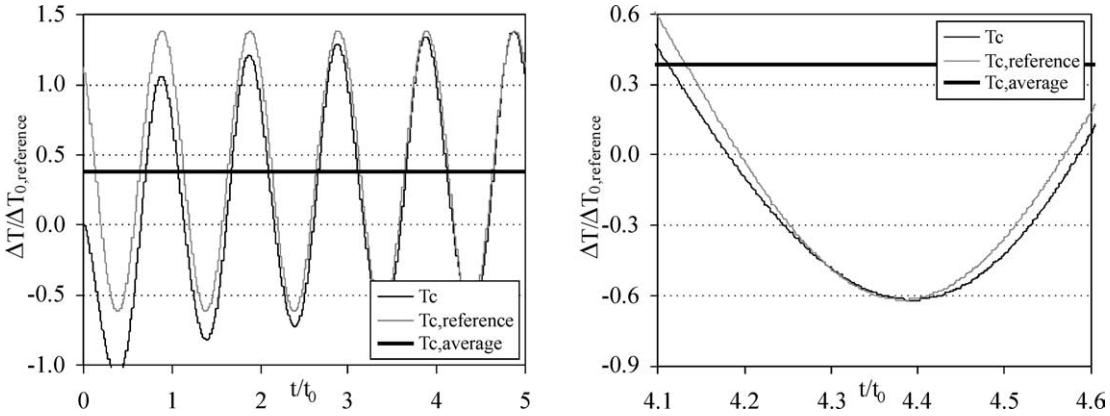

Fig. 5. Time-evolution of ΔT numerically calculated for a harmonic current cycle with zero mean value.

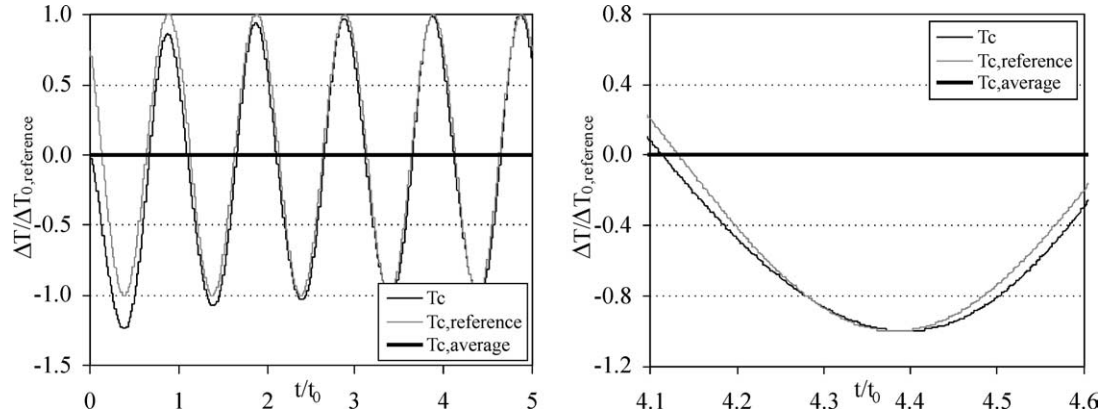

Fig. 6. Time-evolution of ΔT numerically calculated for a harmonic current cycle with above-zero mean value.

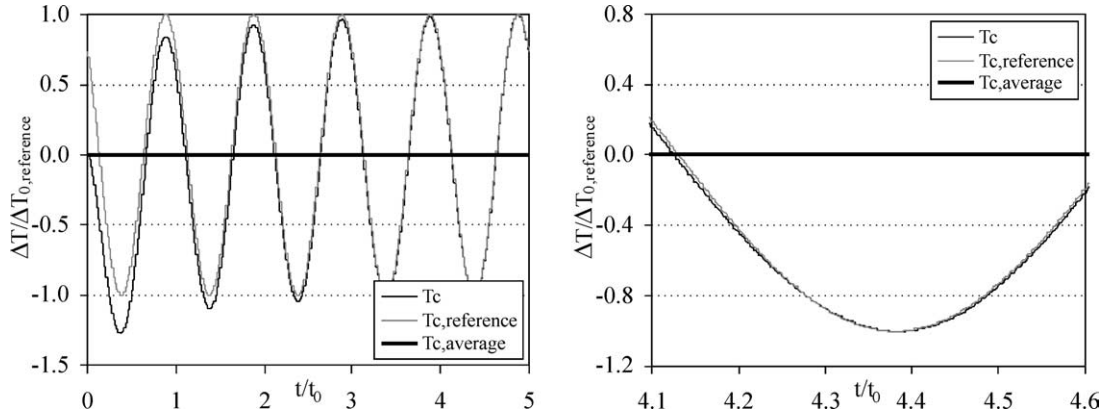

Fig. 7. Time-evolution of ΔT numerically calculated for a harmonic current cycle with different amplitudes in heating and cooling.

The desired time-evolution pattern of the current is given by the acceptable solution of Eq. (16) with respect to I:

$$I(t) = \frac{G}{r}\left[a(T_h - \Delta T) - \sqrt{a^2(T_h - \Delta T)^2 - 2rk\Delta T - r\frac{Q_c}{NG}}\right] \quad (17)$$

The time-dependence of Eq. (17) is in the following terms:

$$\Delta T = \Delta T(t) \quad (18)$$

$$Q_c = Q_c(t) = \frac{d(C\Delta T)}{dt} + Q_{c,ext}(t) \quad (19)$$

If the hot side of the thermoelectric module is kept at ambient temperature, the heat capacity C to be considered is given by half of the module capacity. For a transverse application of the thermal signal, the heat capacity of the portion of specimen below the contact interface must also be added.

The system of Eqs. (17)–(19) can be used to impose not only a harmonic thermal disturbance, but also any

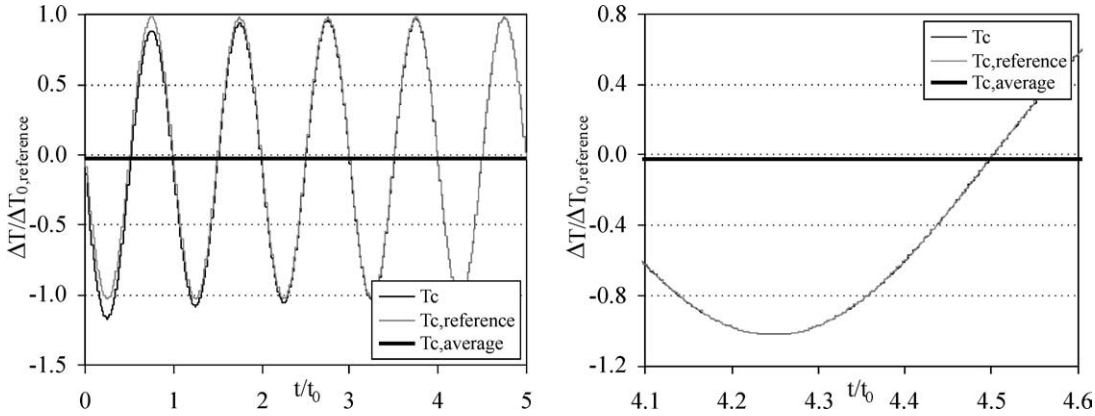

Fig. 8. Time-evolution of ΔT numerically calculated for the analytically-developed current cycle.

other types of time-varying thermal input, provided that the temperature fluctuations are small enough to consider invariable the semiconductor properties and, most of all, that it is possible to define an analytical relationship for the dependence of the external heat load on time and/or temperature. If an estimate of this is possible, a satisfactory thermal input is obtained since from start, and it can be optimized through only a small number of experiments.

In the proposed method, one wants to impose at the input surface the harmonic temperature oscillation described by Eq. (4). The amplitude of the oscillation, ΔT_0, must achieve a compromise between intensity of the thermal signal, which has to be as large as possible, and containment of the effects of non-linear phenomena such as the dependence on temperature of the material properties and the boundary conditions.

One may also presume that the surface temperature of the specimen equals the cold-side temperature of the heat pump. Assuming a null initial phase φ_0 for sake of simplicity, one has:

$$\Delta T(t) = T_a - T_c(t) \cong T_a - T(0,t) = \Delta T_0 \sin\left(2\pi \frac{t}{t_0}\right) \quad (20)$$

A thermal contact resistance exists between heat pump and specimen. A small values of this is however achievable by using a conductive grease and a proper pressure at the contact interface.

The external heat load $Q_{c,ext}$ of the heat pump is actually given by the heat rate flowing through the contact area A between the thermoelectric source and the specimen. For a one-dimensional configuration of the test system, this load can be estimated through some trigonometric transformations as follows:

$$Q_{c,ext}(t) = Ak_s \left.\frac{dT}{dx}\right|_{x=0} = \Delta T_0 A \sqrt{k_s \rho_s c_s \frac{\pi}{t_0}(\beta^2 + \gamma^2)} \times \sin\left[2\pi \frac{t}{t_0} + \tan^{-1}\left(\frac{\beta}{\gamma}\right)\right] \quad (21)$$

Introducing Eqs. (20)–(21) into Eq. (19), one obtains:

$$Q_c(t) = \Delta T_0 C \frac{2\pi}{t_0} \cos\left(\frac{2\pi}{t_0} t\right) + \Delta T_0 A \sqrt{k_s \rho_s c_s \frac{\pi}{t_0}(\beta^2 + \gamma^2)} \times \sin\left[2\pi \frac{t}{t_0} + \tan^{-1}\left(\frac{\beta}{\gamma}\right)\right] \quad (22)$$

One can observe that the thermal inertia of the system is dominated by the heat capacity C alone as long as the effusivity $k_s \rho_s c_s$ of the specimen is small. Unfortunately, this is seldom the case when testing metals or other materials with high values of the thermal conductivity. On the other hand, the measurement of the conductivity is a goal of the proposed measurement method, so that its value is usually unavailable. An initial guess can however be introduced in Eq. (22) and, subsequently, enhanced through a few experiments.

The above-described control strategy has been theoretically tested by predicting the thermal signal for a current cycle governed by Eqs. (17), (20), and (22) through a fully numerical model of the specimen and the thermoelectric heat pump. The temperature distribution along the specimen was calculated numerically by a finite-difference approach. This analysis has yielded excellent outcomes, showing that a perfect signal can be obtained also in case of transverse heat input. Moreover, the temperature estimated at the input interface is virtually coincident with a reference harmonic cycle after only two-three current cycles (see Fig. 8).

Troubles may in practice arise from the constancy of the hot-side temperature of the heat pump, T_h, which should be as close as possible to the test ambient value; a satisfactory steadiness of T_h is however achieved through a liquid-cooled heat-sink and a proper flow rate of coolant from a reservoir at steady temperature. A thorough characterization of the heat pump must also be performed, to determine the exact value of the thermoelectric properties and the cold-side heat capacity.

As for the external heat load, it has been verified that even large errors on the preliminary estimate of the effusivity affect significantly the amplitude of the thermal cycle, but not its harmonic behavior or the average value. Moreover, if the measurement of the diffusivity is the goal of the experiment, the calibration of the external load provides an indirect confirmation to the accuracy of the measured value.

The above-described approach was employed during the most recent stages of the work, where the external heat

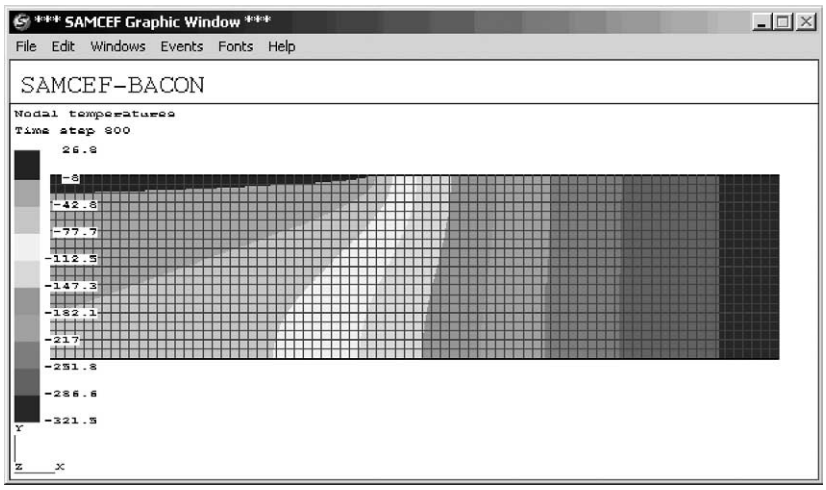

Fig. 9. Instantaneous temperature distribution numerically calculated in the specimen cross-section (Samcef plot).

load of Eq. (21) was neglected, with the encouraging results reported before [1,2,6,7].

4. One-dimensional wave propagation

As previously mentioned, a direct-contact source is used to apply the thermal signal. This makes not easy to achieve an uniform heat input all over the contact interface, since the contact resistance to the heat flux can be inhomogeneous due to surface roughness or imperfect flatness. It is therefore necessary to supply the thermal input on a 'strip' of one of the two main surfaces of the slab specimen, where a homogeneous contact can be yielded by using an adequate contact pressure.

Such a practice, however, implies that the measures of surface temperature are useful to estimate the diffusivity only beyond a certain distance from the input source. In fact, the wave-front of the temperature oscillation is initially plane and parallel to the specimen surface. Then, it starts bending and becoming more and more curved, until a plane wave-front is achieved again, but at this time perpendicular to the specimen surface.

The distance at which the above condition is met, and a true one-dimensional propagation of the thermal signal is yielded aside of the input strip, along the main dimension of the specimen, is investigated here by both numerical and experimental analyses. Through these, a general rule is established for the performance of the experiments.

An extensive numerical investigation was performed, using the finite element code Samcef [22]. The purpose was to compare the accuracy of the equations to estimate the diffusivity, with respect to fully two-dimensional solutions.

The simulation reproduced the slab shown in Fig. 1. A harmonically oscillating temperature profile was imposed onto the thermal input surface. The slab surface temperature was calculated over the remainder of the top face, which would be the optically accessible surface. Convective heat transfer was assumed to occur on all surfaces exposed to air, with a constant convection coefficient and air temperature. The thermo-physical properties of the materials were considered constant.

Despite of the application of the input transversally to the direction of wave propagation, such propagation can be considered one-dimensional at sufficient distance from the source. This can be noticed in Fig. 9, which shows the instantaneous temperature distribution on the cross-section of the slab. The thermal disturbance is applied on the left part of the top surface. The isothermal lines, which represent the thermal waves propagating in the slab, progressively turn into straight vertical lines, as the waves move away from the heat source.

The same behavior of the thermal waves was observed in the experiments. A thermographic image of the instantaneous temperature distribution on the side surface of a specimen is shown in Fig. 10.

A thorough numerical investigation showed that the planar wave-front is fully developed at a distance from the source greater than the specimen thickness, d. This is evident in Fig. 11, which plots the local derivative of the wave phase and the wave amplitude, both normalized to their asymptotic values, versus the normalized distance from the source, x/d. Independently of the thermal diffusion length, L, and of the intensity of convection (in the terms β and γ), the thermal system within the specimen can actually be considered one-dimensional for $x/d > 1$.

Altogether, the numerical and experimental results demonstrate that Eq. (6) is always applicable if the surface-temperature distribution is monitored at a distance from the source greater than d.

It can also be verified by some simple mathematical considerations that the minimum distance from the source is shortened to $d/2$, if a 'sandwich' configuration as in Fig. 12 is used. More specifically, the periodic thermal input can be supplied by two different thermoelectric modules, between which the specimen is sandwiched. This also allows

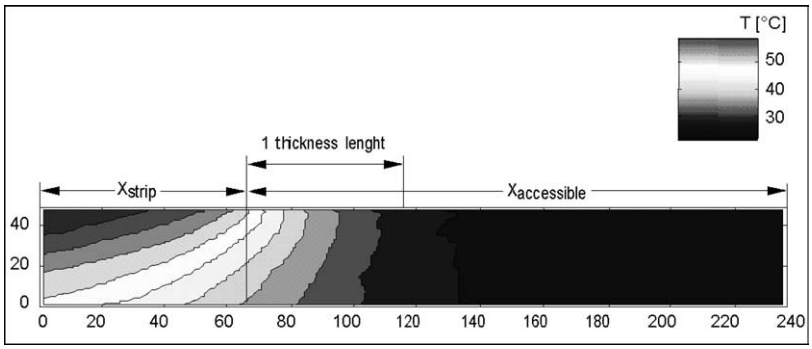

Fig. 10. Instantaneous temperature distribution measured on the specimen side surface (thermographic image) AISI-304 specimen, $d = 1.7$ mm.

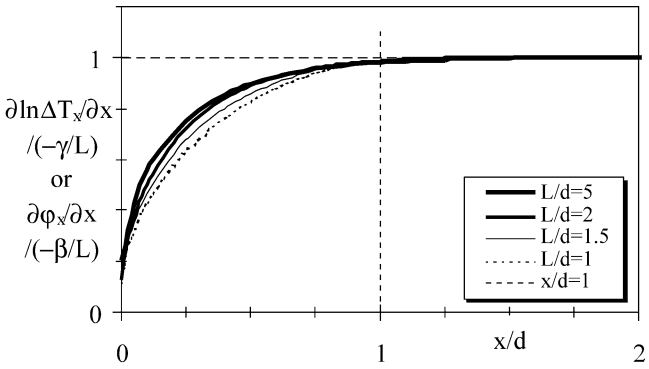

Fig. 11. Wave-phase φ_x and wave-amplitude ΔT_x numerically calculated versus the distance from the source.

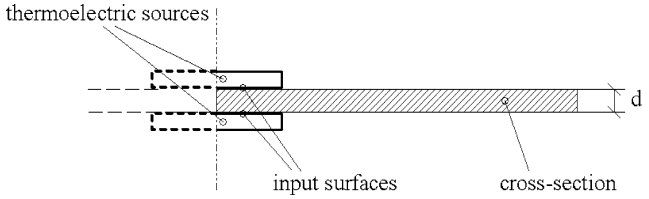

Fig. 12. Slab specimen and thermal source: 'sandwich configuration'.

an easier application of the desired contact pressure and, if necessary, an increase in the maximum amplitude of the thermal heat input. It is only required that the two thermoelectric modules have exactly equal performance, which can be quickly verified through commercial testing devices [23].

5. Concluding remarks

A novel approach to the well-known Ångström's method to measure the thermal diffusivity of solid materials has been developed. This approach is different from other techniques, mostly using photo-thermal sources, in that a harmonic thermal signal is supplied to the specimen by a thermoelectric source based on the Peltier effect. Through this, a steady-periodic propagation of thermal waves with ambient mean value can be obtained in the solid. The thermal diffusivity is then estimated by tracking the thermal wave propagation on the solid surface by infrared thermography.

At the current stage of development, the method is targeted to the case of a thin slab of high-conductivity material, in which a one-dimensional temperature field is easily produced. The harmonic input is applied onto a surface strip that covers the whole width of the slab. The thermal diffusivity is eventually correlated to the phase lag and the exponentially decaying amplitude of the thermal waves propagating along the slab. These are tracked on the same surface where the thermal input is applied, adjacent to the thermal input area.

In this work, the experimental implementation of the test method was investigated, focusing on obtaining a thermal signal both perfectly harmonic and one-dimensional.

A perfectly-harmonic thermal signal permits to recover the diffusivity value by an effortless processing of the experimental data. Moreover, a null net heat input of the signal allows setting the average temperature of the specimen to the ambient value.

The most practical way to obtain null net heat input is employing a thermoelectric source based on the Peltier effect. In fact, this device pumps heat when a direct current flows through it, and it can alternate heating and cooling stages by simply switching the direction of the current.

A harmonic and well-balanced thermal signal can be achieved by supplying to the thermoelectric source a current with a purposely-chosen time-evolution pattern. The pattern can be developed from the analytical formula that governs the transient behavior of a thermoelectric module and its thermal load.

The approach, already tested with satisfactory results, was here improved by enhancing the analytical model on which the time-evolution pattern is obtained. From the enhanced model, a more accurate time-evolution pattern is developed for the current supply, by which an optimal thermal input can theoretically be provided.

Another crucial aspect of the experimental procedure is that the thermoelectric source supplies the thermal signal by direct contact. This makes not easy to achieve an uniform heat input all over the contact interface, due to surface roughness or imperfect flatness. Thus, a homogeneous contact must be assured by using a proper contact pressure. This can be applied by placing the thermal source on one of the two main surfaces of the slab specimen.

This practice implies that the surface-temperature measures are useful to estimate the diffusivity only beyond a certain distance from the input surface, where the wave-front of the temperature oscillation becomes plane and perpendicular to the main surfaces of the specimen. But a thorough investigation, which is here presented, allowed establishing that a true one-dimensional propagation of the signal is yielded at a distance from the source just greater than the specimen thickness, independently of the duration of the signal period and the intensity of the heat transfer between specimen and ambient. Moreover, the distance can be halved by adopting a 'sandwich' architecture of the thermal source.

The research presented here is part of a long-term project, aimed at the full implementation of the proposed approach to the measurement of the thermal diffusivity. The final goal is to overcome some limitations of the most utilized standard test methods, the guarded-hot-plate and the laser flash, in the characterization of thin specimens with high conductivity or diffusivity. In particular, a more accurate characterization is sought than by the guarded-hot-plate, using a much simpler experimental procedure than for the laser flash.

Acknowledgements

This study was made possible by the financial contribution of the Italian M.I.U.R. The authors wish to thank Prof. Giovanni S. Barozzi and Prof. Paolo Tartarini, University of Modena and Reggio Emilia (Italy), and Prof. Antonio C.M. Sousa, University of New Brunswick (Canada), for their inestimable technical advice.

References

[1] A. Muscio, E. Grinzato, The lock-in heating-cooling method for the measurement of the thermal diffusivity of solid materials, Heat Transfer Engineering 23 (2) (2002) 44–52.
[2] A. Muscio, F. Gavelli, P. Tartarini, Measurement of the thermal diffusivity of thin slab specimens by the lock-in heating-cooling method, in: Proceedings of 19th National Heat Transfer Conference, Modena, Italy, 2001, pp. 155–160.
[3] H.S. Carslaw, J.C. Jaeger, Conduction of Heat in Solids, Oxford Univ. Press, Oxford, 1947.
[4] G.S. Barozzi, M.A. Corticelli, A. Muscio, P. Tartarini, Numerical investigation of a one-side measurement technique for thermal diffusivity, in: Proceedings of 17th National Heat Transfer Conference, Ferrara, Italy, 1999, pp. 421–434.
[5] S. Marinetti, P.G. Bison, E. Grinzato, A. Muscio, Thermal diffusivity measurement of stainless steel by periodic heating technique, in: Proceedings of 5th AITA Workshop, Venezia, Italy, 1999, pp. 316–321.
[6] P.G. Bison, S. Marinetti, A. Mazzoldi, E. Grinzato, C. Bressan, Cross-comparison of thermal diffusivity measurements by thermal methods, Infrared Physics and Technology 43 (3–5) (2002) 127–132.
[7] F. Cernuschi, P.G. Bison, S. Marinetti, A. Figari, L. Lorenzoni, E. Grinzato, Comparison of thermal diffusivity measurement techniques, in: Proceedings of Quantitative InfraRed Thermography 6, Dubrovnik, Croatia, September 24–27, 2002, submitted for publication.
[8] Agema Thermovision® 900 Series, User Manual, 1993.
[9] L.C. Aamodt, J.C. Murphy, Photothermal measurements using a localized excitation source, J. Appl. Phys. 52 (8) (1981) 4903–4914.
[10] I. Hatta, Y. Sasuga, R. Kato, A. Maesono, Thermal diffusivity measurement of thin films by means of an AC method, Rev. Sci. Instruments 56 (8) (1985) 1643–1647.
[11] E.P. Visser, E.H. Versteegen, W.J.P. van Enckevort, Measurement of thermal diffusion in thin films using a modulated laser technique: Application to chemical-vapor-deposited diamond films, J. Appl. Phys. 71 (7) (1992) 3238–3248.
[12] H.P.R. Frederikse, R.J. Fields, A. Feldman, Thermal and electrical properties of Copper–Tin and Nickel–Tin intermetallics, J. Appl. Phys. 72 (7) (1992) 2879–2882.
[13] L. Fabbri, P. Fenici, Three-dimensional photothermal radiometry for the determination of the thermal diffusivity of solids, Rev. Sci. Instruments 66 (6) (1995) 3593–3600.
[14] A. Feldman, N.M. Balzaretti, A modification of Angstrom's methods that employs photothermal radiometry to measure thermal diffusivity: Application to chemical vapor deposited diamond, Rev. Sci. Instruments 69 (1) (1998) 237–243.
[15] J.E. Graebnera, H. Altmann, N.M. Balzaretti, R. Campbell, H.-B. Chae, A. Degiovanni, R. Enck, A. Feldman, D. Fournier, J. Fricke, J.S. Goela, K.J. Gray, Y.Q. Gu, I. Hatta, T.M. Hartnett, R.E. Imhof, R. Kato, P. Koidl, P.K. Kuo, T.-K. Lee, D. Maillet, B. Remy, J.P. Roger, D.-J. Seong, R.P. Tye, H. Verhoeven, E. Wörner, J.E. Yehoda, R. Zachai, B. Zhang, Report on a second round robin measurement of the thermal conductivity of CVD diamond, Diamond and Related Materials 7 (1998) 1589–1604.
[16] C.E. Powers, Measuring thermal diffusivity of a high Tc-superconductor, NASA (Goddard Space Flight Center) Technical Brief GSC-13392, USA, 1992.
[17] Y. Gu, X. Tang, Y. Xu, I. Hatta, Ingenious method for eliminating effects of heat loss in measurements of thermal diffusivity by ac calorimetric method, Japan. J. Appl. Phys. 32 (1993) L1365–L1367.
[18] W. Czarnetzki, W. Roetzel, Temperature oscillation techniques for simultaneous measurement of thermal diffusivity and conductivity, Internat. J. Thermophysics 16 (2) (1995) 413–422.
[19] P.G. Bison, A. Muscio, E. Grinzato, Thermal parameters estimation by heating and cooling and thermographic measurement, in: Proceedings of Thermosense XXI SPIE Conference, USA, vol. 3700, SPIE, Orlando, 1999, pp. 402–408.
[20] B.J. Huang, C.L. Duang, System dynamic model and temperature control of a thermoelectric cooler, Internat. J. Refrigeration 23 (2000) 197–207.
[21] K. Uemura, Commercial Peltier modules, in: D.M. Rowe (Ed.), CRC Handbook of Thermoelectrics, CRC Press, 1995, pp. 621–631.
[22] S.A. Samtech, Samcef User Manual, version 7.1.
[23] G. Gromov, D. Kondratiev, A. Rogov, L. Yershova, Z-meter: Easy-to-use application and theory, available online: www.rmtltd.ru.